Calcif Tissue Int (1999) 65:459–465

Calcified Tissue International

A Comparative Infrared Spectroscopic Study of Hydroxide and Carbonate Absorption Bands in Spectra of Shark Enameloid, Shark Dentin, and a Geological Apatite

S. Dahm, S. Risnes

Department of Oral Biology, Faculty of Dentistry, University of Oslo, P.O. Box 1052 Blindern, N—0316 Oslo, Norway

Received: 1 June 1998 / Accepted: 12 March 1999

Abstract. The purpose of the present work was to investigate the infrared (IR) spectrum of shark enameloid, especially with regard to hydroxide and carbonate bands. With thin sections placed directly in the IR beam it was possible to get high concentrations of ions without interfering effects from a dispersion medium (e.g., alkali halides). For comparison, spectra of shark dentin and a geo-apatite were also recorded. In spectra of shark enameloid and geo-apatite medium strong hydroxide absorption bands were found around 3535 cm^{-1}, and in shark dentin and geo-apatite spectra weak shoulders were observed at about 3570 cm^{-1}. Hydroxide libration bands at about 740 cm^{-1} were found in shark enameloid and geo-apatite spectra; in the latter, also a band at 680 cm^{-1}. Carbonate bands were found in shark enameloid spectra at 1480 (weak shoulder), 1453, 1423, and 868 cm^{-1}. In shark dentin spectra there were carbonate bands at 1452, 1417, and 875 cm^{-1}, and probably also a carbonate band at about 1530 cm^{-1} overlapped by an amide II band. Weak carbonate bands were also found in the spectra of the geo-apatite at 1452 cm^{-1}, and at about 1425 and 880 cm^{-1}. The relative intensities of the bands at 1453 cm^{-1} (contributed from A and B sites) and around 1420 cm^{-1} (B sites) changed from shark enameloid to shark dentin, and also from shark enameloid to the geo-apatite. More A sites seem to be occupied by carbonate in shark dentin than in shark enameloid, supposedly owing to fluoride occupation of A sites in shark enameloid. In geo-apatite and shark enameloid there are hydroxide ions hydrogen bonded to fluoride. Both shark enameloid and the geo-apatite are fluoride rich, and geo-apatite seems to have the highest fluoride concentration. There are, however, indications that the hydroxide concentration is also higher in the geo-apatite than in shark enameloid. This can be explained by the much higher carbonate content, and partly also by the higher water content in shark enameloid. There are A sites in geo-apatite and probably also in shark enameloid which are occupied by carbonate, but the proportion of occupied A sites relative to occupied B sites is greater in geo-apatite than in shark enameloid. This difference can be explained by the preference of A sites when the carbonate concentration is very low. On the other hand, for greater amounts of carbonate such as we have in shark enameloid, B sites are preferred.

Key words: Infrared spectroscopy — Enameloid — Apatite — Carbonate — Hydroxide.

Correspondence to: S. Dahm

The biological apatite constituting the crystals in the mineralized tissues (bone and teeth) of amphibians, reptiles, and mammals, is mostly poor in fluoride. However, in shark enameloid, which is analogous to dental enamel in higher vertebrates, the hydroxide ion sites in the hydroxyapatite structure are occupied by a substantial amount of fluoride [1–9], thus resulting in a biological fluorapatite. Shark enameloid contains carbonate, though in lesser amounts than in human enamel [1, 5, 7, 9]. Carbonate ions may substitute at two different sites in the hydroxyapatite crystal lattice: for hydroxide (A sites), and for phosphate (B sites) [10–13]. These three types of substitutions in the hypothetical hydroxyapatite structure—fluoride for hydroxide, carbonate for hydroxide, and carbonate for phosphate—are suitable for infrared (IR) spectroscopy study.

Studying thin crystal sections of Durango fluorapatite by IR spectroscopy, Levitt and Condrate [14] observed an absorption band at 3535 cm^{-1}. They used polarized radiation and found that the band had maximum intensity with the polarizing plane parallel to the c axis in the crystal. This was interpreted to mean that Durango fluorapatite must have some "impurity" hydroxide ions in the crystals. The powder spectra (alkali halide discs) of this apatite do not normally exhibit hydroxide bands [15]. Since the normal hydroxide stretching mode for hydroxyapatite is at 3570 cm^{-1}, this means that Durango fluorapatite has its hydroxide ions hydrogen bonded to neighboring fluoride ions in a linear chain along the c axis [16–24]. Levitt and Condrate [14] also found a shoulder at 3480 cm^{-1}, which is probably due to OH^-–Cl^- hydrogen bonding [16, 17, 20]. In spectra of geological fluorapatites and synthetic hydroxyfluorapatites so-called "librational bands" in the region 750–630 cm^{-1} have also been observed due to librational motions of the hydroxide ion, more or less weakly hydrogen bonded to fluoride [20, 21, 25].

Elliott [26] studied polarized IR spectra of francolite, tooth enamel, and synthetic carbonate apatites and found that carbonate gave rise to absorption bands at 1545, 1450, and 880 cm^{-1} for A type, and at 1465, 1412, and 873 cm^{-1} for B type substitution. There are many different absorption frequencies reported in the literature for pure A type, pure B type, and AB type. The position of the absorption bands in AB type also depends on the amount of carbonate substitution [24, 27] and the degree of fluoride substitution in fluorcarbonate apatites [11, 24]. A compilation of wave numbers from the literature gives the following wave number regions for absorption bands: 1552–1534 cm^{-1}, 1472–

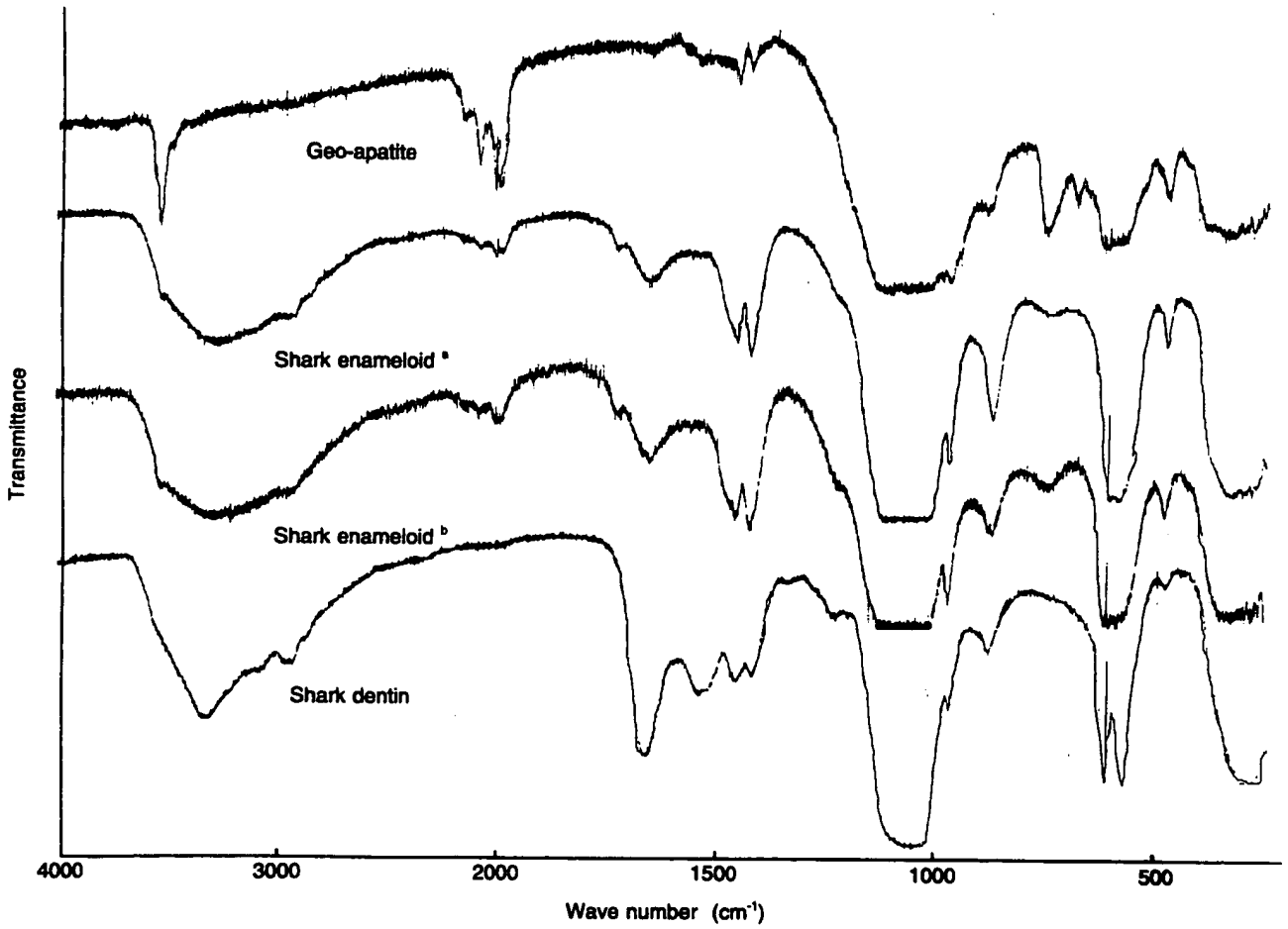

Fig. 1. IR spectra of thin sections of geo-apatite (45 μm), shark enameloid (10 μm), and shark dentin (6–7 μm). The geo-apatite and the shark dentin spectrum were recorded with the widest slit program. The two enameloid spectra (from the same tooth and section, middle enameloid) were recorded with the widest (a) and with the normal (b) slit program, respectively; spectrum (a) is ordinate-expanded relative to spectrum (b).

1450 cm^{-1}, 883–878 cm^{-1} for A sites, and 1465–1450 cm^{-1}, 1430–1410 cm^{-1}, 874–862 cm^{-1} for B sites [11, 12, 24, 26, 28–35]. Note that in the 1465–1450 cm^{-1} region there is an overlap between A and B bands [26, 30].

The aim of the present work was to record IR spectra of mature shark enameloid by a technique similar to that of Levitt and Condrate [14], and further to compare these spectra with IR spectra of shark dentin and a geological fluorapatite, focusing on hydroxide and carbonate absorption bands. Shark dentin contains about the same amount of carbonate, but much less fluoride than enameloid [2, 5, 6], and the geological apatite has a high content of fluoride, but very little carbonate. Thereby, a foundation is made for assignments and comparison of intensities of absorption bands, and accordingly to draw conclusions regarding the crystal structure.

With thin sections placed directly in the IR beam, the concentration of ions will be higher than in alkali halide discs, and the interfering effects of alkali halide (adsorbed water, opaque discs) will be avoided.

Materials and Methods

The material consisted of fully developed teeth from *Isurus oxyrinchus* (Mako shark or Mackerel shark) and a geological fluorapatite (green-blue crystals) from Kragerø, Norway [36].

The main bulk of crystallites in shark enameloid is oriented parallel with the enameloid surface [37].

The enameloid layer had a thickness of about 500 μm [38]. Seven sections with thicknesses of about 300 μm, containing only enameloid, were obtained by preparing tangential surface sections [39] from seven different shark teeth. The sections were further reduced in thickness by grinding according to a modified version of the method of Sundstrøm [40] using silicon carbide paper with water until a thickness of 25–75 μm was reached. By varying the amount of grinding from the dentinal and/or the superficial aspect of the section, the final section represented either the outer, middle, or inner part of the enameloid. After recording IR spectra of the sections, three of the sections were ground further to 10–30 μm: two of these sections were from the outer and middle enameloid, respectively, and both were about 25 μm before and 10 μm after the last grinding. IR spectra were again recorded. A tangential section of shark dentin was ground to 25–30 μm thickness and IR spectra were recorded. This section was further ground to 6–7 μm and IR spectra were again recorded. One section of geo-apatite was ground to a thickness of 45 μm. Because of the fragility of the sample it was not possible to get this section thinner. IR spectra were recorded. During grinding, the sections were glued to a brass cylinder with Histokitt® (Assistant-Germany), which afterwards was dissolved by soaking in xylene.

Infrared Spectroscopy

A Perkin-Elmer spectrophotometer model 457 was used for the recording of IR spectra.

As the sections used in the present study were cut parallel to the surface, the main mass of crystals were consequently oriented perpendicular to the analyzing beam. But the orientation of the crystals relative to the slit varied between samples. Sheets of radially directed crystals are also present in the enameloid. This minor component of crystals were thus oriented parallel with the analyzing beam. Though unpolarized radiation was used, gratings themselves can act as polarizers. No attempt was made to observe such effects.

The area of the ground sections (about 2 × 4 mm) was less than the cross-section of the beam. The sections were therefore masked with paper frames and aluminum strips and placed in a disc holder so that no part of the beam that did not pass through the sections was allowed to reach the detector. Because of this the transmittance scale had to be expanded by placing wire gauze or a comb attenuator in the reference beam. The amplifier gain setting of the instrument therefore had to be increased, and this led to a higher electronic noise level. To minimize the noise, the widest slit program (twice the normal program energy) was used in most of the spectra. This setting corresponds to approximately 1.5 times the normal slit width, and therefore a greater signal-to-noise ratio is obtained, though with reduced resolution (6 cm^{-1} at 3000 cm^{-1}, and 3 cm^{-1} at 1000 cm^{-1}).

The spectra were scanned at the slowest scanning speed—100 cm^{-1}/minute in the range 4000–2000 cm^{-1}, and 50 cm^{-1}/minute in the range 2000–250 cm^{-1}. Expressed in the centimeter unit, the scan speed is 1.0 cm/minute, and the scanning of one whole spectrum lasts for 55 minutes.

To minimize interference from atmospheric bands (CO_2 and H_2O), the spectrophotometer was flushed with dry nitrogen during most of the recordings.

The absorption bands of polystyrene film, atmospheric water vapor, and carbon dioxide were used to calibrate the spectra. The wave number accuracy of sharp bands was estimated to be ±5 cm^{-1} in the 4000–2000 cm^{-1} region, and ±2 cm^{-1} in the 2000–250 cm^{-1} region.

From each of the shark enameloid sections, 1–11 spectra were recorded, from the shark dentin section 13 spectra were recorded, and from the geo-apatite section 6 spectra were recorded.

Results

Figure 1 shows selected spectra of thin sections of geo-apatite (~45 μm), shark enameloid (~10 μm), and shark dentin (6–7 μm). The geo-apatite and dentin spectra shown were recorded with the widest slit program, and the two enameloid spectra shown were recorded with the normal and the widest slit program, respectively.

Hydroxide (OH^-) Absorption Bands

Stretching Modes. The shark enameloid spectra showed a shoulder at about 3530 cm^{-1}. The spectra of geo-apatite showed a medium strong absorption band at about 3540 cm^{-1}, with weak shoulders at 3570 and 3480 cm^{-1}. A very weak shoulder at about 3570 cm^{-1} was observed in some shark dentin spectra.

Librational Modes. The spectra from four of the enameloid sections showed a weak, broad absorption band at 740 cm^{-1}. The spectra of geo-apatite showed a medium strong absorption band at 745 cm^{-1}, and a weaker band at 680 cm^{-1}. In the region 750–630 cm^{-1} no absorption bands were observed in the shark dentin spectra.

Carbonate (CO_3^{2-}) Absorption Bands

Stretching Modes. Of the enameloid sections, one section from the inner enameloid gave a very weak absorption band at about 1540 cm^{-1}. This was the only section from the inner enameloid. A very weak absorption band was observed at 1540 cm^{-1} in three spectra of a 25 μm-thick section from the outer enamel. In the shark dentin spectra, there was a weak broad band at 1540–1520 cm^{-1}. In one spectrum of geo-apatite a very weak absorption band at 1540 cm^{-1} was observed.

In spectra from five of the enameloid sections a very weak shoulder at about 1480 cm^{-1} was observed, but nothing at this position was observed in the spectra of shark dentin and geo-apatite.

The absorption band at 1453 cm^{-1} was at the same wavenumber for all sections [perhaps with a small lowering (1452 cm^{-1}) in the shark dentin and the geo-apatite section].

The band which averaged 1423 cm^{-1} in the spectra of shark enameloid shifted to 1417 cm^{-1} in the shark dentin spectra. The corresponding band in the geo-apatite spectra was approximately at 1425 cm^{-1} (high noise level).

It is noteworthy that the relative intensities of the bands at 1453 cm^{-1} (contributed from A and B site) and around 1420 cm^{-1} (B site) changed from shark enameloid to shark dentin; in the enameloid spectra the lower wavenumber band was the more intense, whereas in the shark dentin spectra the band with the higher wavenumber was the more intense. In the geo-apatite spectra the relative intensities of the bands at 1425 cm^{-1} and 1453 cm^{-1} were also reversed compared with shark enameloid; furthermore, these bands were weak compared with shark dentin and enameloid.

Deformational Modes. In the enameloid spectra there was one clear carbonate absorption band at 868 cm^{-1}. In one enameloid (middle enameloid) spectrum, where the normal slit program was used, a broad band was observed, which suggests "splitting" (Fig. 1). In other spectra of the same specimen, where the wide slit program was used, faint shoulders were observed at 875 cm^{-1} (Fig. 1). The main band shifted to about 875 cm^{-1} in shark dentin. In the spectra of geo-apatite, a very weak band was observed at about 880 cm^{-1}.

Other Absorption Bands of Interest

The phosphate bands in the 1150–1000 cm^{-1} region were too strong (due to sections that were too thick) to reveal the details in the bands, especially in the shark enameloid and the geo-apatite spectra (off scale). For shark dentin, strong phosphate bands were observed at 563 and 602 cm^{-1}. The corresponding bands for enameloid and geo-apatite were often too strong to be observed, but in some spectra bands were observed at about 575 cm^{-1}. Other phosphate bands were observed at 965 and 471 cm^{-1} (averaged) in all spectra; the differences between samples and between sections were too small to be considered significant. Note also the bands in the 2200–1900 cm^{-1} region, most distinct in the spectrum of geo-apatite.

In all enameloid spectra, "water bands" were observed: a very broad and medium-to-strong band at about 3280 cm^{-1},

and a medium band at about 1650 cm^{-1}. The latter also appeared as a very faint band in the spectrum of the geo-apatite.

Absorption bands of presumably organic origin appeared in both the enameloid and shark dentin spectra in the region 2980–2925 cm^{-1}, and at about 1225 cm^{-1} (as weak shoulders in the enameloid spectra). In the shark dentin spectra there were additional bands at 3330, 3160–3080, 1660 cm^{-1}, about 1530 cm^{-1} (broad), and at 1332 cm^{-1}, reflecting the higher organic content in this tissue.

A weak band at 1730 cm^{-1}, of which the authors have no ready explanation, was observed only in the enameloid spectra. The possibility that this band arises from the adhesive (Histokitt) cannot be excluded.

Discussion

The shoulder at 3530 cm^{-1} in the enameloid spectra and the medium strong band at 3540 cm^{-1} in the spectrum of the geo-apatite are evidently due to stretching vibrations of hydroxide ions hydrogen bonded to fluoride ions along the c axis in the apatite crystals. Since one-sided OH^-–F^- hydrogen bonds have shorter hydrogen bonds and longer O–H bonds than two-sided OH^-–F^-–HO^- hydrogen bonds, the hydroxide stretching frequencies will be higher in the two-sided configuration than in the one-sided configuration [41, 42]. In accordance with this, the frequency of the dominating hydrogen-bonded hydroxide stretching band in synthetic hydroxyfluorapatites has been found to increase with increasing OH^- concentration [43]. Thus, the difference between the two stretching frequencies at 3530 and 3540 cm^{-1} in the enameloid and geo-apatite spectra, respectively, can be ascribed to a higher concentration of OH^- ions relative to fluoride in the geo-apatite. However, the possibility that the difference may be due to the overlap/interference with the broad water band in the enameloid spectra should be considered.

The weak shoulders observed at 3570 cm^{-1} in shark dentin and geo-apatite are interpreted as the normal stretching mode due to nonhydrogen-bonded OH^- ions along the c axis. The weak shoulder at 3480 cm^{-1} was found only in the geo-apatite spectra, and is probably due to the OH^-–Cl^- bond, as mentioned earlier.

In spectra of synthetic hydroxyfluorapatites, Fowler [20] observed hydroxide librational bands at 735, 715, and 670 cm^{-1} and found that each of these frequencies tended to increase with increasing F^--concentration (or decreasing OH^--concentrations), i.e., an opposite shift of what is observed for stretching frequencies. This is in accordance with the vibration characteristics of the hydrogen bond [42]. No band at 715 cm^{-1} was observed in the present work, neither in the geo-apatite nor in the enameloid spectra. Fowler also found that the band intensities varied with the F^- (and OH^-) content: when $F^- > OH^-$, the 735 cm^{-1} band predominates; when $F^- < OH^-$, the 715 and 670 cm^{-1} predominate. The hydroxide libration bands around 740 cm^{-1} found in the enameloid and geo-apatite spectra are in agreement with these samples being fluoride rich, and are probably due to one-sided OH^-–F^- hydrogen bonds (single OH^--ions in an extended F^--column) [20, 21]. In line with the same reasoning, the band at 680 cm^{-1} in the geo-apatite spectra could be due to the two-sided OH^-–F^-–HO^- hydrogen bonds [16, 43]. The reason a band at 670–680 cm^{-1} did not show up in the shark enameloid spectra may be that enameloid is relatively poor in hydroxide compared with the geo-apatite, so that the ratio F^-/OH^- is higher in enameloid than in the geo-apatite, and accordingly, provided the ions are distributed at random along the c axis [22], the OH^-–F^-–HO^- configuration will be less probable, and the OH^-–F^- configuration more probable in enameloid than in the geo-apatite. Freund and Knobel [21] assigned the band at 680 cm^{-1} to a "tail-to-tail" (···HO:OH···) configuration. These authors also found a band at 3643 cm^{-1}, which they assigned to the same configuration. This band has not been observed by others, nor by the present authors, and most probably arises from a $Ca(OH)_2$ impurity [22, 43].

The reason that no other hydroxide bands than the band at 3570 cm^{-1} were observed in the shark dentin spectra is evidently due to the much lower fluoride content (few possibilities for hydrogen bonding to fluoride). The weakness of the 3570 cm^{-1} band, and the absence of the librational band at 630 cm^{-1} [21], could be due to the smaller and more imperfect apatite crystallites in shark dentin [44]. It could also imply that there are few hydroxide ions in shark dentin. Rey et al. [33] found practically no hydroxide ions in AB type carbonate apatite synthesized in solution at pH 7.5, nor in bone mineral [45].

The carbonate bands at 1452 and 1425 cm^{-1} in the geo-apatite spectra and at 1453 and 1423 cm^{-1} in the enameloid spectra indicate that there is about the same fluoride concentration in shark enameloid and in the geo-apatite—perhaps a little more in the geo-apatite [9, 11, 24, 43]. The bands at 740 cm^{-1} and 745 cm^{-1} in the enameloid and geo-apatite spectra, respectively, indicate that the geo-apatite has a significantly higher fluoride content than enameloid [20, 21], provided that the other ions/molecules/vacancies along the c-axis in the apatite crystals do not influence the position of this librational absorption band to an appreciable extent. Thus, it seems that the geo-apatite has a higher concentration of both fluoride and hydroxide than shark enameloid. A possible explanation could be the difference in carbonate content: there is obviously much more carbonate in shark enameloid than in the geo-apatite, as indicated by the difference in band intensities in the regions 1550–1350 cm^{-1} and 900–800 cm^{-1} (Fig. 1); consider also that the geo-apatite section is both thicker and more transparent than the enameloid section from which the spectra were recorded. Some of this carbonate may be in A sites, and more in the enameloid than in the geo-apatite. There may also be hydroxide ion vacancies in enameloid due to imperfections in the hydroxyapatite lattice introduced by substitution of carbonate in *B sites* [32, 45]. The spectra in Figure 1 show that there is a substantial amount of water in enameloid as opposed to the geo-apatite (regions 3800–2500 cm^{-1} and 1700–1600 cm^{-1}). Some of this water may be substituted for OH^- in A sites, as in human enamel [43, 46].

In a detailed IR study of OH^- hydrogen-bonded to F^- in synthetic hydroxyfluorapatites, Freund and Knobel found an absorption band at 745 cm^{-1} and a weaker band at 680 cm^{-1} at 76 mol % F– (of total $OH^- + F^-$ in hydroxyfluorapatite) [21]. This corresponds well with the spectra of geo-apatite in the present study. Freund and Knobel also observed a faint shoulder at 720 cm^{-1}, which may explain the unsymmetrical shape of the absorption band at 745 cm^{-1} for the geo-apatite in the present study. It therefore seems reasonable to assume that the fluoride content in the geo-apatite used in the present study is about 75 mol % of the total A sites in the apatite crystals. The absorption band at 740 cm^{-1} in the enameloid spectra should correspond to a fluoride content of about 65 mol % of the total A sites in the

enameloid apatite crystals [21]. This, as pointed out earlier, is on the assumption that other ions/molecules/vacancies along the c-axis have a minor influence on the position of this librational band.

Since both shark enameloid and the geo-apatite are fluoride rich, with a large part of the A sites occupied by fluoride, it was at first assumed that their carbonate was mainly in B sites. Shark dentin, on the other hand, is poor in fluoride, so its carbonate was expected to be in both A and B sites. Hence, shark enameloid and the geo-apatite should be mainly B type apatites and shark dentin should be more AB type. However, as will emerge from the ensuing discussion, the present results indicate that carbonate substitution in A sites also occurs in shark enameloid and geo-apatite, and to a relatively greater degree in geo-apatite.

The shift of the carbonate stretching band at 1417 cm^{-1} and the carbonate deformational band at 875 cm^{-1} in the shark dentin spectra to 1423 cm^{-1} and 868 cm^{-1}, respectively, in the shark enameloid spectra can be associated with the higher fluoride content in shark enameloid [9, 11, 24, 33, 43, 47].

The broad band at about 870 cm^{-1} in the spectrum of middle enameloid recorded with the normal slit program, and the faint shoulder observed at about 875 cm^{-1} alongside the dominating band at 868 cm^{-1} in spectra of middle enameloid recorded with the wide slit program (Fig. 1), suggest the presence of two closely positioned absorption bands. IR spectra of synthetic partially fluoridated carbonate apatites [24, 47] are in accordance with this suggestion. Two closely positioned bands in this region may indicate that carbonate occupies both A and B sites. This agrees with what the present authors hypothesized related to the OH^- content in enameloid, namely, that there are A sites in enameloid that are occupied by carbonate. The reason that two closely positioned absorption bands at about 875 cm^{-1} were not observed in spectra of shark dentin, in spite of more A sites "available" for carbonate than in enameloid, may be the low crystallinity or the low fluoride content [24] compared with enameloid. Two absorption bands at 878 and 871 cm^{-1}, indicating that carbonate substitution had occurred in both A and B sites, were observed by Rey et al. [33] in deconvoluted FTIR spectra of bone and in spectra of fluoride-free AB type samples synthesized in solution at pH 7.5, but these authors undoubtedly had a better resolution in their spectra than in the present work.

The broad band at 1540–1520 cm^{-1} in the shark dentin spectra is probably composed of an A site carbonate band and an amide II band [48]. Also, one geo-apatite spectrum showed a very weak band at 1540 cm^{-1}. From one section (about 25 μm thick) of the outer enamel there is probably a very weak band at 1540 cm^{-1} which appeared in three of four spectra. The reason that bands were not observed in this position in spectra of *middle enameloid* sections, nor from the 25 μm section may be bad quality of the spectra. Only two spectra were recorded of this section, and maximal ordinate expansion (the baseline was between 0.2–0.4 in absorbance units) was not achieved. It must also be taken into consideration that the enameloid samples may show small differences with regard to fluoride, hydroxide, and carbonate content. The very weak absorption band at 1540 cm^{-1} detected from a section of the inner enameloid may be ascribed to A site carbonate because of lower fluoride concentration than in the middle enameloid [9], but it could also be due to carbonate/amide II from dentin extensions into the enameloid [38].

The difference in the relative intensities of the 1453 and the 1420 cm^{-1} bands between the shark dentin and shark enameloid spectra agrees with findings in spectra of natural [49] and synthetic fluor-carbonate apatites and carbonate apatites [11, 47, 50, unpublished]. A possible explanation for this difference is that, since the band at 1453 cm^{-1} has contributions from carbonate in both A and B sites, it will be relatively weaker in enameloid spectra due to a large amount of fluoride in A sites in enameloid. Thus, these observations support the expectation that in shark dentin there are more A sites filled with carbonate than in enameloid. It is also interesting that the same relative intensities of the bands at 1453 and 1420 cm^{-1} as in shark enameloid have been observed in spectra of synthetic apatites which were claimed to be B type carbonate apatites without fluoride [24, 33, 51]. A spectrum of a representative sample prepared at pH 9 and with a carbonate content of 4.1% showed no band at 1550–1540 cm^{-1}, and bands at 1454, 1421, and 875 cm^{-1} [51]. A spectrum of another sample prepared at a fluctuating pH 5–9 and with a carbonate content of 0.7%, about the same as Glas [1] found in shark dentin, showed bands at 1550, 1455, 1418, and 874 cm^{-1} [51]. The intensities of the bands at 1455 and 1418 cm^{-1} in the second sample were about equal, whereas in the first sample the band at 1421 cm^{-1} was distinctly more intense than the band at 1454 cm^{-1}. Thus, the spectrum from the second sample is closer to the spectrum of shark dentin, which corroborates that the mineral phase in shark dentin is an AB type apatite. The shift of the carbonate stretching band at 1418 cm^{-1} in the spectrum of the second sample to 1421 cm^{-1} for the first sample is in the same direction as from shark dentin to enameloid. On the other hand, the carbonate deformational band at 875 cm^{-1} did not show any significant shift, as opposed to the shift from 875 to 868 cm^{-1} in the spectra of shark dentin and enameloid, respectively. It seems that this band, which is dependent on the fluoride content, is relatively independent of changes from AB type to B type in fluoride-free apatites [24].

If the geo-apatite should be mainly a B type apatite, as expected to begin with in the present work, a B site band at 868 cm^{-1} (as in enameloid) or lower [11, 43] would be anticipated in the spectra, perhaps with a weak shoulder at a higher wave-number as in enameloid. This was not the case. Instead, a band at about 880 cm^{-1} in the geo-apatite spectra was observed which was rather puzzling. Contrary to the original expectation, it seems that the geo-apatite is not mainly a B type apatite but nearer to an A type, in spite of its high fluoride content (it should be mentioned that the band at 880 cm^{-1} and the shoulder at 875 cm^{-1} in the geo-apatite and shark enameloid spectra, respectively, are very poorly defined, so the difference may be nonsignificant). A possible explanation is that when the carbonate concentration is low, as in geo-apatite, A sites are preferred [24, 32, 52]. This is confirmed by the relative intensities of the 1452 and 1425 cm^{-1} band (Fig. 1), and also agrees with the weak band at 1540 cm^{-1} observed in one spectrum of geo-apatite [33]. When the carbonate concentration increases, the proportion of occupied B sites increases [24, 32], as in shark enameloid.

The weak shoulder at about 1480 cm^{-1} observed in the enameloid spectra is supposedly of the B type [24, 32].

The 563 cm^{-1} band should be typical for a hydroxyapatite-resembling lattice [15, 53–55], and the 575 cm^{-1} band should be typical for a fluorapatite-resembling lattice [15, 49, 54]. This is in accordance with the shark dentin being F^--poor and the shark enameloid and the geo-apatite being F^--rich. We have also recorded powder spectra of "our"

geo-apatite, which show the same phosphate bands as Durango apatite, which is established as a relatively pure fluorapatite [15]. However, in addition, at about the same concentration in the disc as Durango apatite, our geo-apatite spectrum shows bands at 3540 and 745 cm^{-1}. This suggests that there is a higher concentration of OH^--ions in our geo-apatite than in Durango apatite.

The bands in the 2200–1900 cm^{-1} region have been assigned to phosphate overtone and combination bands [15, 20]. The bands at 3280 and 1650 cm^{-1} arise from stretching and bending modes in the water molecule [29, 56, 57].

Acknowledgement. Our thanks to Dr. Berit Johne for the gift of several samples of a geological apatite found in the surrounding country of Kragerø.

References

1. Glas J-E (1962) Studies on the ultrastructure of dental enamel. VI. Crystal chemistry of shark's teeth. Odontologisk Revy 13:313–326
2. Büttner W (1966) Konzentration und Verteilung von Fluorid in Haifischzähnen. Adv Fluor Res Dent—Car Prevent 4:193–200
3. Petersson LG, Frostell G (1974) Secondary ion microanalysis of fluorine in apatites of biological interest. Z Naturforsch 29c:417–420
4. Møller IJ, Melsen B, Jensen SJ, Kirkegaard E (1975) A histological, chemical and X-ray diffraction study on contemporary (*Carcharias glaucus*) and fossilized (*Macrota odontaspis*) shark teeth. Arch Oral Biol 20:797–802
5. LeGeros RZ, Suga S (1980) Crystallographic nature of fluoride in enameloids of fish. Calcif Tissue Int 32:169–174
6. Suga S (1982) Fluoride concentration in the teeth of cartilaginous fishes (Chondrichthyes) (abstract). J Dent Res 61:255
7. LeGeros RZ, Silverstone LM, Daculsi G, Kerebel LM (1983) In vitro caries-like lesion formation in F-containing tooth enamel. J Dent Res 62:138–144
8. Suga S, Ogawa M (1989) Comparative observations on trace element distribution in enamel and enameloid. In: Fearnhead RW (ed) Tooth enamel V. Florence Publishers, Tsurumi, Yokohama, pp 353–359
9. Miake Y, Aoba T, Moreno EC, Shimoda S, Prostak K, Suga S (1991) Ultrastructural studies on crystal growth of enameloid minerals in Elasmobranch and Teleost fish. Calcif Tissue Int 48:204–217
10. Bonel G (1972) Contribution a l'étude de la carbonatation des apatites. Part I. Ann Chim 7:65–88
11. Bonel G (1972) Contribution a l'étude de la carbonatation des apatites. Parts II and III. Ann Chim 7:127–144
12. Santos M, González-Díaz PF (1977) A model for B carbonate apatite. Inorg Chem 16:2133–2134
13. González-Díaz PF, Santos M (1979) McConnells' model vs. the $HPO_4 \rightarrow CO_3$ model for carbonate apatite. Inorg Chem 18:899–900
14. Levitt SR, Condrate Sr RA (1970) The polarized infrared spectra of hydroxyl ion in fluorapatite. Appl Spectroscopy 24:288–289
15. Baddiel CB, Berry EE (1966) Spectra structure correlations in hydroxy and fluorapatite. Spectrochim Acta 22:1407–1416
16. Young RA, van der Lugt W, Elliott JC (1969) Mechanism for fluorine inhibition of diffusion in hydroxyapatite. Nature 223: 729–730
17. Dykes E, Elliott JC (1971) The occurrence of chloride ions in the apatite lattice of Holly Springs hydroxyapatite and dental enamel. Calcif Tissue Res 7:241–248
18. Engel G, Klee WE (1972) Infrared spectra of the hydroxyl ions in various apatites. J Solid State Chem 5:28–34
19. Amberg CH, Luk HC, Wagstaff KP (1974) The fluoridation of nonstoichiometric calcium hydroxyapatite. An infrared study. Can J Chem 52:4001–4006
20. Fowler BO (1974) Infrared studies of apatites. I. Vibrational assignments for calcium, strontium, and barium hydroxyapatites utilizing isotopic substitution. Inorg Chem 13:194–207
21. Freund F, Knobel RM (1977) Distribution of fluorine in hydroxyapatite studied by infrared spectroscopy. J Chem Soc Dalton Trans 1136–1140
22. Baumer A, Ganteaume M, Klee WE (1985) Determination of OH ions in hydroxyfluorapatites by infrared spectroscopy. Bull Minér 108:145–152
23. Bigi A, Foresti A, Ripamonti A, Roveri N (1986) Fluoride and carbonate incorporation into hydroxyapatite under condition of cyclic pH variation. J Inorg Biochem 27:31–39
24. Shimoda S, Aoba T, Moreno EC, Miake Y (1990) Effect of solution composition on morphological and structural features of carbonated calcium apatites. J Dent Res 69:1731–1740
25. Montel G, Heughebaert JC (1978) Influence of fluoride ions on calcium orthophosphates hydrolysis. In: Courvoisier B, Donath A, Baud CA (eds) Second symposium CEMO, fluoride and bone. Hans Huber Publishers, Bern, Stuttgart, Vienna, pp 82–93
26. Elliott JC (1965) The interpretation of the infra-red absorption spectra of some carbonate-containing apatites. In: Stack MV, Fearnhead RW (eds) Tooth enamel. John Wright, Bristol, pp 20–22
27. Elliott JC, Holcomb DW, Young RA (1985) Infrared determination of the degree of substitution of hydroxyl by carbonate ions in human dental enamel. Calcif Tissue Int 37:372–375
28. Trombe JC, Bonel G, Montel G (1968) Sur les apatites carbonatées préparées à haute températures. Bull Soc Chim France Numéro Spécial 1708–1712
29. Holcomb DW, Young RA (1980) Thermal decomposition of human tooth enamel. Calcif Tissue Int 31:189–201
30. Young RA, Bartlett ML, Spooner S, Mackie PE (1981) Reversible high temperature exchange of carbonate and hydroxyl ions in tooth enamel and synthetic hydroxyapatite. J Biol Phys 9:1–26
31. Driessens FCM, Verbeeck RHM, Heijligers HJM (1983) Some physical properties of Na- and CO_3-containing apatites synthesized at high temperatures. Inorg Chim Acta 80:19–23
32. Vignoles M, Bonel G, Holcomb DW, Young RA (1988) Influence of preparation conditions on the composition of Type B carbonated hydroxyapatite and on the localization of the carbonate ions. Calcif Tissue Int 43:33–40
33. Rey C, Collins B, Goehl T, Dickson IR, Glimcher MJ (1989) The carbonate environment in bone mineral: a resolution-enhanced Fourier transform infrared spectroscopic study. Calcif Tissue Int 45:157–164
34. Aoba T, Moreno EC (1990) Changes in the nature and composition of enamel mineral during porcine amelogenesis. Calcif Tissue Int 47:356–364
35. Mayer I, Schneider S, Sydney-Zax M, Deutsch D (1990) Thermal decomposition of developing enamel. Calcif Tissue Int 46:254–257
36. Neumann H (1985) The minerals of Norway. Norges geologiske undersøkelser skrift 68. Universitetsforlaget Trondheim, p 119
37. Risnes S (1990) Shark tooth morphogenesis—An SEM and EDX analysis of enameloid and dentin development in various shark species. J Biol Buccale 18:237–248
38. Risnes S, Fosse G (1979) Serially etched shark enameloid observed by incident light microscopy. Acta Anat 105:1–8
39. Risnes S (1981) A rotating specimen holder for hard tissue sectioning. Stain Technol 56:265–266
40. Sundström B (1966) A technique of preparing thin ground sections of hard tissues: tooth and bone. Acta Odontol Scand 24:159–178
41. Van der Lugt W, Knottnerus DIM, Young RA (1970) NMR determination of fluorine position in mineral hydroxyapatite. Caries Res 4:89–95
42. Hadži D, Bratos S (1976) Vibrational spectroscopy of the hydrogen bond. In: Schuster P, Zundel G, Sandorfy C (eds)

The hydrogen bond. North-Holland Publishing Company, Amsterdam, New York, Oxford, p 565
43. Elliott JC (1994) Structure and chemistry of the apatites and other calcium orthophosphates. Elsevier, Amsterdam, London, New York, Tokyo
44. LeGeros RZ (1981) Apatites in biological systems. Prog Crystal Growth Charact 4:1–45
45. Rey C, Miquel JL, Facchini L, Legrand AP, Glimcher MJ (1995) Hydroxyl groups in bone mineral. Bone 16:583–586
46. LeGeros RZ, Bonel G, Legros R (1978) Types of "H_2O" in human enamel and in precipitated apatites. Calcif Tissue Int 26:111–118
47. Okazaki M (1983) F^-–CO_3^{2-} interaction in IR spectra of fluoridated CO_3^{2-}-apatites. Calcif Tissue Int 35:78–81
48. Rao CNR (1963) Chemical applications of infrared spectroscopy. Academic Press, New York, London, p 524
49. Evans LA, Macey DJ, Webb J (1992) Calcium biomineralization in the radular teeth of the Chiton, *Acanthopleura hirtosa*. Calcif Tissue Int 51:78–82
50. Okazaki M (1991) Crystallographic behaviour of fluoridated hydroxyapatites containing Mg^{2+} and CO_3^{2} ions. Biomaterials 12:831–835
51. Apfelbaum F, Diab H, Mayer I, Featherstone JDB (1992) An FTIR study of carbonate in synthetic apatites. J Inorg Biochem 45:277–282
52. Callens FJ, Verbeeck RMH, Naessens DE, Matthys PFA, Boesman ER (1993) ESR study of ^{13}C-enriched carbonated calciumapatites precipitated from aqueous solutions. Calcif Tissue Int 52:386–391
53. Menzel B, Amberg CH (1972) An infrared study of the hydroxyl groups in a nonstoichiometric calcium hydroxyapatite with and without fluoridation. J Coll Interface Sci 38:256–264
54. McCarty DJ, Lehr JR, Halverson PB (1983) Crystal populations in human synovial fluid. Identification of apatite, octacalcium phosphate, and tricalcium phosphate. Arthritis Rheum 26:1220–1224
55. Mitchell PCH, Parker SF, Simkiss K, Simmons J, Taylor MG (1996) Hydrated sites in biogenic amorphous calciumphosphates: an infrared, raman, and inelastic neutron scattering study. J Inorg Biochem 62:183–197
56. Corbridge DEC, Lowe EJ (1954) The infra-red spectra of some inorganic phosphorus compounds. J Chem Soc 493–502
57. Iijima M, Kamemizu H, Wakamatsu N, Goto T, Moriwaki Y (1991) Thermal decomposition of Lingula shell apatite. Calcif Tissue Int 49:128–133